

- Acta, **31**, 171, (1973).
- (27) Sometimes these "secondary" factors become more important than the "primary" electronic ones. See, for instance, the discussion in C. J. Marsden and L. S. Bartell, *Inorg. Chem.*, **15**, 3004 (1976); L. S. Bartell, F. B. Clippard, and E. J. Jacob, *ibid.*, **15**, 3009 (1976).
- (28) (a) True, this trend in overlap populations of the C-F is also connected with the antibonding contributions of the C-F π bonds,²² a factor not entering in the explicit form in our model. This illustrates difficulties of a direct use of sophisticated calculations for checking any model using another (usually simpler) formalism. See the discussion of this aspect in ref 2 and 9c. (b) The CNDO/2 calculations on the $CF_{4-k}H_k$ series (D. P. Brown, cited in ref 18, p 95) do not agree with the ab initio ones²² in the C-F bond population trend.
- (29) F. A. Cotton and G. Wilkinson, "Advanced Inorganic Chemistry", 3rd ed., Interscience, New York, N.Y., 1972, p 310.
- (30) See, for instance, ref 4a, p 219.
- (31) For a detailed discussion see ref 25.
- (32) This conclusion is valid for both σ and π bonding. Numerous examples of such π bonding can be found in the linear $L'-M-L$ fragments of $ML_{m-k}L'_k$ complexes where the d_{π} metal orbitals do not interact with the σ ligand orbitals, say d_{xz} , d_{yz} , d_{xy} orbitals in quasi-octahedral complexes $ML_{6-k}L'_k$ (cf. Figure 3b),^{9,33,34}
- (33) (a) E. M. Shustorovich, Yu. A. Buslaev, and Yu. V. Kokunov, *Zh. Strukt. Khim.*, **13**, 111 (1972); (b) E. M. Shustorovich, M. A. Poray-Koshits, T. S. Khodasheva, and Yu. A. Buslaev, *ibid.*, **14**, 706 (1973).
- (34) (a) J. I. Zink, *J. Am. Chem. Soc.*, **94**, 8039 (1972); (b) *ibid.*, **96**, 4464 (1974).
- (35) This fact is a keystone of the $3o-3c-4e$ model itself.^{4a,9b,36-40}
- (36) (a) G. C. Pimentel, *J. Chem. Phys.*, **19**, 446 (1951); (b) G. C. Pimentel and R. D. Spratley, *J. Am. Chem. Soc.*, **85**, 826 (1963).
- (37) (a) R. J. Hach and R. E. Rundle, *J. Am. Chem. Soc.*, **73**, 4321 (1951); (b) R. E. Rundle, *ibid.*, **85**, 112 (1963); (c) *Rec. Chem. Prog.*, **23**, 195 (1962).
- (38) E. E. Havinga and E. H. Wibenga, *Recl. Trav. Chim. Pays-Bas*, **78**, 724 (1959).
- (39) H. H. Hyman, Ed., "Noble-Gas Compounds", University of Chicago Press, Chicago, Ill., 1963, Chapter 9.
- (40) Reference 29, pp 109-111.
- (41) Some strong hydrogen bonds $X-H\cdots Y$ may be included here as well, but usually weak asymmetric bonds $X-H\cdots Y$ are not the object of the $3o-4c$ model (see discussion in ref 42).
- (42) P. A. Kollmann in "Applications of Electronic Structure Theory", H. F. Schaefer III, Ed., Plenum Press, New York, N.Y., 1977, Chapter 3.
- (43) N. W. Alcock, *Adv. Inorg. Chem. Radiochem.*, **15**, 1 (1972).
- (44) I. D. Brown, *J. Solid State Chem.*, **11**, 214 (1974).
- (45) O. Foss, *Pure Appl. Chem.*, **24**, 31 (1970).
- (46) J.-S. Lee, D. D. Titus, and R. F. Ziolo, *J. Chem. Soc., Chem. Commun.*, 501 (1976).
- (47) (a) O. Vikane, *Acta Chem. Scand., Ser. A*, **29**, 738 (1975); (b) S. Hauge and O. Vikane, *ibid.*, **29**, 755 (1975); (c) O. Vikane, *ibid.*, **29**, 763 (1975); (d) *ibid.*, **29**, 787 (1975).
- (48) J. D. McCullough, *Inorg. Chem.*, **14**, 1142 (1975).
- (49) K. W. Hansen and L. S. Bartell, *Inorg. Chem.*, **4**, 1775 (1965).
- (50) (a) EHM and CNDO/2: J. M. Howell, *J. Am. Chem. Soc.*, **97**, 3930 (1975). (b) Ab initio: F. Keil and W. Kutzelnigg, *ibid.*, **97**, 3623 (1975), and references cited therein.
- (51) E. M. Shustorovich, to be submitted for publication.
- (52) See, for instance, ref 36-39, 43-45.
- (53) For example, a great number of the relevant molecules have been calculated by ab initio methods,⁵⁴ not to mention the countless semiempirical calculations like those in ref 38 and 39.
- (54) W. G. Richards, T. E. H. Walker, L. Farnell, and P. R. Scott, "Bibliography of ab initio Molecular Wave Functions. Supplement for 1970-1973", Clarendon Press, Oxford, 1974.
- (55) In linear ALL' and planar trigonal $AL_3-kL'_k$ compounds where A has vacant valence p_{π} orbitals, the A-L bonds may even be strengthened by a better σ donor L' owing to donor-acceptor $\pi_L \rightarrow \pi_A$ interactions if L' is not a π donor (such as H or CH_3) but L is a good π donor (such as I or Br).

Generalized Berlin Diagram for Polyatomic Molecules

T. Koga,[†] H. Nakatsuji,* and T. Yonezawa

Contribution from the Department of Hydrocarbon Chemistry,
Faculty of Engineering, Kyoto University, Kyoto, Japan. Received March 16, 1978

Abstract: The region-functional concept of electron density, which was first presented by Berlin for diatomic molecules (Berlin diagram), is explicitly generalized for polyatomic molecules on the basis of the electrostatic Hellmann-Feynman theorem. For a given internal coordinate (process), the space around the molecule is separable into accelerating (A) and resisting (R) regions (generalized Berlin diagram). The electron density in the A region accelerates the process, while the density in the R region resists it. The generalized Berlin diagram thus gives an explicit regional definition useful for the density-guiding rule for nuclear-rearrangement processes. The generalized Berlin diagrams are illustrated for the three internal modes of H_2O and are superposed on the density difference maps. They are shown to give a basis for clarifying the density origin of the geometry and vibration.

Introduction

In recent years, the force and density approaches based on the electrostatic Hellmann-Feynman (H-F) theorem¹ have received much attention in molecular quantum chemistry.² The primary advantage of the force concept lies in its simplicity and visually compared with those of the energetics. Furthermore, the H-F forces are directly connected with the electron density of a system, so that the forces along the process are mainly governed by the behavior of the electron density along the process.^{3,4} From this point of view, we have given previously a density-guiding rule for nuclear-rearrangement processes, based on intuition for the region-functional roles of the electron density along the process.⁴

In 1951, Berlin considered the region-functional role of the electron density for diatomic molecules.⁵ He divided the molecular space into binding and antibinding regions. Namely, the electron density in the binding region gives a force which binds the two nuclei, while the density in the antibinding region

gives a force which separated the nuclei. At the equilibrium internuclear distance, the binding force just balances with the sum of the antibinding force and the nuclear repulsion. For diatomic molecules, Bader et al.^{6a} and others^{6b} have studied the nature of chemical bonds using the Berlin diagram superposed on the electron density and density difference maps.

For polyatomic molecules, Bader^{7a} and Johnson⁸ have "synthesized" generalized Berlin diagrams by superposing the diatomic Berlin diagrams for the bonds included in a molecule. Bader and Preston^{7b} have also considered a different superposition. Though they have obtained some intuitive results from such diagrams, their method seems to be less general. Indeed, it would be difficult to get a region-functional diagram for a bending mode, a twisting mode, etc. from such a simple modification of the diatomic Berlin diagram.

A purpose of this paper is to generalize unambiguously Berlin's region-functional concept of electron density to any internal coordinates of polyatomic molecules. We will use the center-of-mass-of-the-nuclei (CMN) coordinates, instead of the geometric-center-of-the-nuclei (GCN) coordinates used

[†] Department of Industrial Chemistry, Muroran Institute of Technology, Muroran, Japan.

by Berlin. The latter is obtained as a special case of the former. We first consider the case of diatomic molecules and then extend the idea to polyatomic molecules. In the generalized Berlin diagram, the space around the molecule is divided into accelerating (A) and resisting (R) regions with respect to the process along any internal (symmetry and normal) coordinates of a molecule. It defines explicitly the regions for the density-guiding rule.⁴ We illustrate the generalized Berlin diagrams for the three symmetric coordinates of the triatomic AB₂ molecules. We superpose these diagrams on the electron density of H₂O and show how these diagrams actually work in studying the geometry of molecule.

Binding and Antibinding Regions in the CMN Coordinates

We consider the binding force in a diatomic molecule AB which has nuclei A and B and electrons {i}. Though Berlin considered the binding force using the GCN coordinates, it seems adequate to use the CMN coordinates since the internal motions in many-particle systems are more appropriately described in the CMN coordinates. In the following, we briefly compare the binding forces in the CMN and GCN coordinates and show the binding and antibinding regions in the CMN coordinates.

We first compare the momenta in both coordinates, from which the force operators are derived. The momenta \mathbf{P}_R conjugate to the internuclear vector \mathbf{R} are given by

$$\mathbf{P}_R(\text{CMN}) = (m_A \mathbf{P}_B - m_B \mathbf{P}_A) / (m_A + m_B) \quad (1a)$$

$$\mathbf{P}_R(\text{GCN}) = (\mathbf{P}_B - \mathbf{P}_A) / 2 + (\mathbf{P}_A + \mathbf{P}_B + \sum_i \mathbf{P}_i) (m_A - m_B) / 2M \quad (1b)$$

where \mathbf{P} 's on the right-hand side represent the momenta of nuclei and electrons, m is the nuclear mass, and M is the mass of the molecule. Equation 1 shows that in the CMN coordinates, \mathbf{P}_R is the difference in the nuclear momenta with mass factors, but in the GCN coordinates, it includes the external translational momentum except for the homonuclear case (the second term). The binding force operators \mathcal{F}_R are obtained from the commutation of the electronic Hamiltonian H and the momenta \mathbf{P}_R , $\mathcal{F}_R = i[H, \mathbf{P}_R]$.⁹ They are

$$\mathcal{F}_R(\text{CMN}) = (m_A \mathcal{F}_B - m_B \mathcal{F}_A) / (m_A + m_B) \quad (2a)$$

$$\mathcal{F}_R(\text{GCN}) = \mathcal{F}_R(\text{CMN}) + (\mathcal{F}_A + \mathcal{F}_B) (m_B - m_A) / 2(m_A + m_B) \quad (2b)$$

where \mathcal{F}_A and \mathcal{F}_B mean the force operators for the nuclei A and B, respectively. In contrast to the operator $\mathcal{F}_R(\text{CMN})$, $\mathcal{F}_R(\text{GCN})$ includes the operator of the external translational force ($\mathcal{F}_A + \mathcal{F}_B$) except for homonuclear diatomics ($m_A = m_B$). This is due to the fact that in the GCN coordinates, the internal motion is not well separated from the external motion. Therefore, the CMN coordinates seem to be more suitable than the GCN coordinates for the study of the binding force (internal force) in diatomic molecules. Using the force operators (eq 2) with the electron density $\rho(\mathbf{r}_1)$, we obtain the binding forces as

$$F_R = \langle \mathcal{F}_R \rangle = - \int f \rho(\mathbf{r}_1) d\mathbf{r}_1 + Z_A Z_B / R^2 \quad (3)$$

where f is the electronic part of the force operator given by

$$f(\text{CMN}) = \frac{1}{m_A + m_B} \{ m_B (Z_A \cos \theta_A / r_{A1}^2) + m_A (Z_B \cos \theta_B / r_{B1}^2) \} \quad (4a)$$

$$f(\text{GCN}) = \frac{1}{2} \{ (Z_A \cos \theta_A / r_{A1}^2) + (Z_B \cos \theta_B / r_{B1}^2) \} \quad (4b)$$

Here, Z is nuclear charge, r_{A1} the distance between the electron 1 and the nucleus A, and θ_A the angle between the vectors

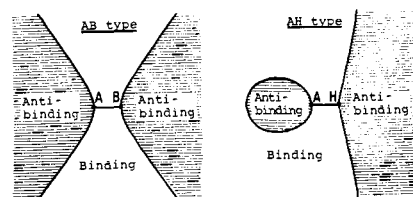


Figure 1. Binding and antibinding regions in the CMN coordinates.

r_{A1} and \mathbf{R} . For the floating or stable wave functions,¹⁰ the binding forces F_R obtained in both coordinates coincide with each other. However, the operator $f(\text{CMN})$ is different from $f(\text{GCN})$, which was derived by Berlin,⁵ so that the resultant binding-antibinding diagram in the CMN coordinates is different from the original Berlin diagram.

As in the Berlin diagram, the binding and antibinding regions in the CMN coordinates are divided by the surface $f(\text{CMN}) = 0$.¹¹ The boundary surface depends on masses and charges. Since the ratio Z/m is unity (au/amu) for hydrogen and approximately $1/2$ for the other atoms, the binding-antibinding diagrams in the CMN coordinates are classified approximately into two and *only* two types, an AB type and an AH (hydride) type, where AB means all of the homo- and heteronuclear diatomics except for the hydrides.¹² This is not true for the Berlin diagram (the diagram in the GCN coordinates) in which the boundary surface varies according to the ratios of the nuclear charges Z_A/Z_B . The AB- and AH-type diagrams in the CMN coordinates are shown in Figure 1. These diagrams are the same as the special cases of the Berlin diagram; i.e., the present diagram for AB molecules coincides with Berlin's homonuclear case and that for hydrides with Berlin's heteronuclear case with $Z_A/Z_B = 1/2$. We expect that the present diagrams will be useful in the interpretation of diatomic chemical bonds as well as the Berlin diagram.

Generalization for Polyatomic Molecules

In this section, we consider a generalization of the region-functional concept of Berlin to polyatomic molecules using the H-F forces in the internal coordinates. Here we follow closely the FG matrix method.¹³ For a polyatomic molecule (or a molecular system), we consider the transformation from Cartesian coordinates $\{\mathbf{X}, \mathbf{x}\}$ to internal coordinates $\{\mathbf{R}, \mathbf{r}\}$, where \mathbf{X} and \mathbf{R} denote the nuclear coordinates and \mathbf{x} and \mathbf{r} the electronic coordinates. The coordinates $\{\mathbf{R}\}$ mean the nuclear internal coordinates such as bond lengths, bond angles, out-of-plane angles, torsional angles, etc., and their linear combinations. They are obtained from the Cartesian coordinates as

$$\mathbf{R} = \mathbf{S}\mathbf{X} \quad (5a)$$

$$\mathbf{r} = (-1/M)\mathbf{M}\mathbf{X} + \mathbf{x} \quad (5b)$$

where \mathbf{S} is the S vector defined by $\mathbf{S} = d\mathbf{R}/d\mathbf{X}$, M the mass of the molecule, and \mathbf{M} the matrix whose element is nuclear mass $(\mathbf{M}')_{ij} = m_j$. The first term on the right-hand side of (5b) follows from the choice of the origin of the electronic coordinates at the center of mass of the nuclei. The internal momenta $\{\mathbf{P}_R, \mathbf{P}_r\}$ conjugate to $\{\mathbf{R}, \mathbf{r}\}$ are obtained from the momenta in the Cartesian coordinates $\{\mathbf{P}_X, \mathbf{P}_x\}$ as

$$\mathbf{P}_R = \mathbf{G}^{-1}\mathbf{S}\mathbf{M}^{-1}\mathbf{P}_X \quad (6a)$$

$$\mathbf{P}_r = \mathbf{P}_x \quad (6b)$$

where \mathbf{G} is the inverse kinetic energy matrix ($\mathbf{G} = \mathbf{S}\mathbf{M}^{-1}\mathbf{S}$) and \mathbf{M} is the diagonal nuclear mass matrix.¹³ From (6a), the force operators $\{\mathcal{F}_R\}$ for the internal coordinates $\{\mathbf{R}\}$ are obtained as

$$\mathcal{F}_R = i[H, \mathbf{P}_R] = \mathbf{G}^{-1}\mathbf{S}\mathbf{M}^{-1}\mathcal{F}_X \quad (7)$$

where $\{\mathcal{F}_X\}$ mean the force operators in the Cartesian coordinates. Then the internal forces are given by

$$\begin{aligned} \mathbf{F}_R &= \langle \mathcal{F}_R \rangle \\ &= \int \mathbf{f}_R \rho(\mathbf{r}_1) d\mathbf{r}_1 + \text{nuclear part} \end{aligned} \quad (8)$$

where

$$\mathbf{f}_R = \mathbf{G}^{-1} \mathbf{S} \mathbf{M}^{-1} \mathbf{f}_X \quad (9)$$

The vector \mathbf{F}_R is the column vector whose element is the force along the internal coordinate R . The operators \mathbf{f}_R and \mathbf{f}_X mean the electronic parts of the force operators \mathcal{F}_R and \mathcal{F}_X , respectively.

Equation 8 means that for the internal coordinate R under consideration, the space around the molecule can be divided into two different parts according to their different region-functional roles. Since the electron density $\rho(\mathbf{r}_1)$ is always positive (or zero), the electronic part (the first term) in (8) is positive if $f_R > 0$ and negative if $f_R < 0$. The positive force accelerates the nuclear rearrangement along the coordinate R , whereas the negative force resists the rearrangement. Consequently, we may define the region where $f_R > 0$ as the *accelerating (A) region* and the region where $f_R < 0$ as the *resisting (R) region (generalized Berlin diagram)*. The A and R regions are separated by the boundary surface $f_R = 0$, which depends on the internal coordinates, nuclear charges, masses, and molecular geometry. Generally, the boundary surface passes through the nuclear positions and is planar in the vicinity of the nuclei (see, for instance, Figures 3–5). When we discuss the A–R regions for bond stretching and bending modes, the regions may be referred to as binding-antibinding and bending-linearizing regions, respectively.

The present formulation of the generalized Berlin diagram is applicable to any internal, symmetry, and normal coordinates of any polyatomic molecule and molecular systems. An interesting example is reaction coordinates. When we imagine a nuclear-rearrangement process along such a coordinate, the density reorganization which accumulates more electron density in the A region will contribute to accelerate the process, but the reverse flow of the electron density will contribute to resist the process. This is what the density-guiding rule implies.⁴ In the vicinity of the moving nuclei, the values of the operator f_R in eq 8 are large, and, further, the regions in the direction of the coordinate always belong to the A region and those in the reverse direction to the R region. Therefore, the former reorganization has been called previously as the electron-cloud preceding and the latter as the electron-cloud incomplete following.⁴ Thus, the generalized Berlin diagram gives an explicit definition of the regions for the electron-cloud preceding and incomplete following. Since these dynamic behaviors of the electron density have been shown to occur commonly in any nuclear-rearrangement processes including molecular geometries and chemical reactions,^{3,4,14,15} the generalized Berlin diagram will be useful for studying the density origins of such processes.

Within the framework of the molecular orbital (MO) theory, the electron density of a system is represented as the sum of the MO densities. When the generalized Berlin diagram is applied to the MO density, further information may be obtained. Superposing the diagram on the MO densities, each MO may be distinguished whether it is accelerating or resisting in nature.^{6,16,17} The changes in molecular geometry induced by the changes in the electronic structure such as excitations, ionizations, and electron attachments are also accounted for under the frozen-orbital approximation. An excitation from a resisting MO to an accelerating MO piles up the electron density in the A region and reduces the density in the R region, and hence it will cause the nuclear rearrangement in the direction of the coordinate, and vice versa. An ionization from

a resisting MO or an electron attachment to an accelerating MO will also induce a similar change in molecular geometry, and vice versa. Such a concept has been shown to be useful in predicting the changes in geometries accompanied by excitations and ionizations.^{16,18} The effect of orbital relaxation following such changes in electronic structure has also been examined.^{17,19} The generalized Berlin diagram proposed here would be useful for these studies of molecular geometries.

Diagrams in Other Coordinates

Here, we note that the generalized Berlin diagram in other coordinate systems are easily obtained as a special case of the preceding formulation for the CMN coordinates. The diagram in the GCN (geometric-center-of-the-nuclei) coordinates is obtained from the preceding formulation simply by making all of the nuclear masses equal, i.e.,

$$m_A = m_B = \dots \quad (\text{GCN}) \quad (10)$$

The superposed Berlin diagrams used by Bader^{7a} and Johnson⁸ are obtained by this procedure. A different coordinate system is the one in which the origin of the coordinates is fixed on a special nucleus A in the molecule or on a specially chosen center of the two or three nuclei in the molecule (e.g., the midpoint between equivalent nuclei A and B).²⁰ These coordinates may be called nuclear-centered (NC) coordinates. The diagram in the NC coordinates is obtained from the preceding formulation simply by letting

$$m_A = \infty \quad (\text{NC on A}) \quad (11a)$$

for the former case and

$$m_A = m_B = \infty \quad (\text{NC on a point between A and B}) \quad (11b)$$

for the latter case.

Though different diagrams are obtained depending on the different choice of the coordinate system since the force operator itself is dependent on the choice of the coordinate system, we recommend the CMN coordinates since they are the ones appropriate for the description of the internal motion of molecules and molecular systems. In the coordinates other than the CMN coordinates, the force operator includes in general the operator of the external translational force. However, it is, of course, true that if we use the floating or stable wave function, the external translational force vanishes identically after integration, and any choice of coordinates gives an equivalent result.

Application to Triatomic Molecules

We consider the generalized Berlin diagrams in the CMN coordinates for a nonlinear triatomic molecule AB_2 which has the bond length $r_1 = r_2 = r$ and the bond angle ϕ (see Figure 2). The diagrams for the three symmetry coordinates $2^{-1/2}(r_1 + r_2)$, ϕ , and $2^{-1/2}(r_1 - r_2)$, are considered.

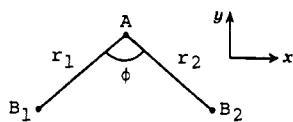
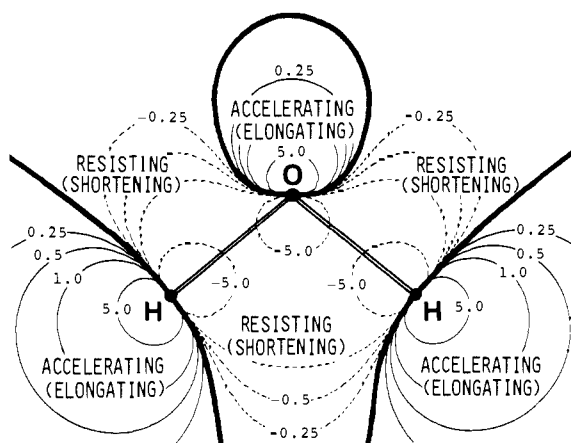
In Table I, we have summarized the force operators corresponding to these symmetry coordinates. The required transformation matrix $\mathbf{G}^{-1} \mathbf{S} \mathbf{M}^{-1}$ was obtained analytically.²¹ There, the operator f_{x1} in the electronic part denotes the x -directional operator of the force on the B_1 nucleus, and m and Z represent the nuclear mass and charge, respectively.

From these force operators, we obtain the generalized Berlin diagrams for the three symmetry coordinates. In Figures 3–5, we show the diagrams for the equilibrium H_2O molecule.²² Figure 3 depicts the generalized Berlin diagram for the totally symmetric stretching mode. The lone-pair region above O and the regions behind the H's along the O–H bonds are shown to be the A region. The intermediate region which involves the two O–H bonds is the R region. Figure 4 shows the diagram for the bending mode. The regions just below O and outer sides

Table I. Force Operators for the Symmetry Coordinates in AB₂ Molecules^{a,b}

mode	force operator	
	electronic, f_R	nuclear
$\frac{1}{\sqrt{2}}(r_1 + r_2)$	$\frac{1}{\sqrt{2}} [s(f_{x2} - f_{x1}) + \frac{c}{m_A + 2m_B} \{2m_B f_{yA} - m_A(f_{y1} + f_{y2})\}]$	$\frac{Z_B(Z_B + 4sZ_A)}{2\sqrt{2}sr^2}$
$r\phi$	$\frac{1}{2} [c(f_{x2} - f_{x1}) + \frac{s}{m_A + 2m_B} \{m_A(f_{y1} + f_{y2}) - 2m_B f_{yA}\}]$	$\frac{cZ_B^2}{4s^2r^2}$
$\frac{1}{\sqrt{2}}(r_1 - r_2)$	$\frac{1}{\sqrt{2}(m_A + 2s^2m_B)} [2sm_B f_{xA} - sm_A(f_{x1} + f_{x2}) - cm_A(f_{y1} - f_{y2})]$	0

^a $s = \sin(\phi/2)$ and $c = \cos(\phi/2)$. ^b The operator f_{x1} in the electronic part denotes the x -directional operator of the force on B₁ nucleus, and m and Z represent the nuclear mass and charge, respectively.

**Figure 2.** Coordinate system for AB₂ molecules.**Figure 3.** Generalized Berlin diagram for the totally symmetric stretching mode of H₂O. Contour values are in e/Å² units.

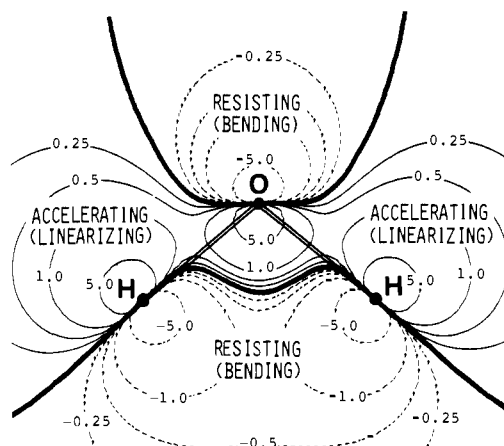
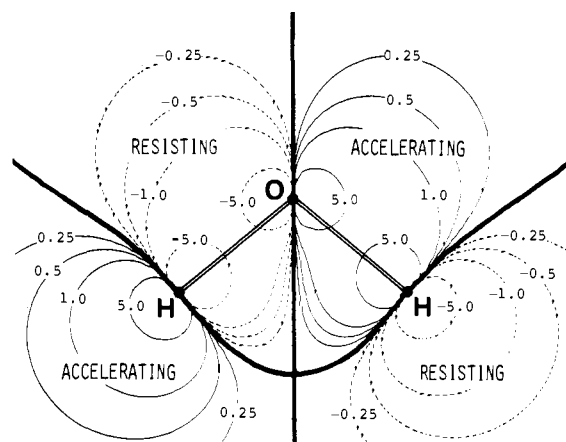
of the O–H bonds are the A region (linearizing region), while the lone-pair region of O and the trapezoidal region below H's are the R region (bending region). The generalized Berlin diagram for the antisymmetric stretching mode is shown in Figure 5. The A and R regions are antisymmetric with respect to the mirror plane. On the left-hand side, the bond region is resisting and the region below H is accelerating.

In the regions near the nuclei, these diagrams show the patterns which are easily expected by intuition. Moreover, as the contour values show, the density *near* the nucleus is important to the H–F force acting on that nucleus. On these grounds, the intuitive ideas hitherto used by many authors may be justified. However, there is also a region for which such intuition may find difficulty. For example, in Figure 4, the region inside of the HOH triangle includes both the A and R regions. The contour lines near the boundary still have a large weighting f_R values. We expect that such a situation will occur more frequently for more complex polyatomic systems.

Geometry of H₂O Molecule

In this section, we discuss the geometry of the H₂O molecule superposing the generalized Berlin diagrams on the density difference maps. We use the density difference $\Delta\rho$ defined by^{23,24}

$$\Delta\rho = \rho_{\text{H}_2\text{O}} - \{\rho_{\text{O}} + \rho_{\text{H}} + \rho_{\text{H}}\}$$

**Figure 4.** Generalized Berlin diagram for the bending mode in the equilibrium H₂O molecule. Contour values are in e/Å² units.**Figure 5.** Generalized Berlin diagram for the antisymmetric stretching mode in the equilibrium H₂O molecule. Contour values are in e/Å² units.

It gives the change in the electron density due to the molecular formation from the separated atoms. We have used the difference $\Delta\rho$ instead of the total density $\rho_{\text{H}_2\text{O}}$, since the latter is inconvenient to see the small changes in the electron density induced by the small displacement around the equilibrium geometry. We consider the nuclear displacements along the three internal coordinates given in the preceding section.

For the totally symmetric stretching mode, the $\Delta\rho$ maps superposed on the generalized Berlin diagram are shown in Figure 6. The density difference has been calculated from the floating wave function reported previously.¹⁴ In the $\Delta\rho$ maps, the solid and broken lines mean the increase and decrease of the electron density relative to the sum of the atomic densi-

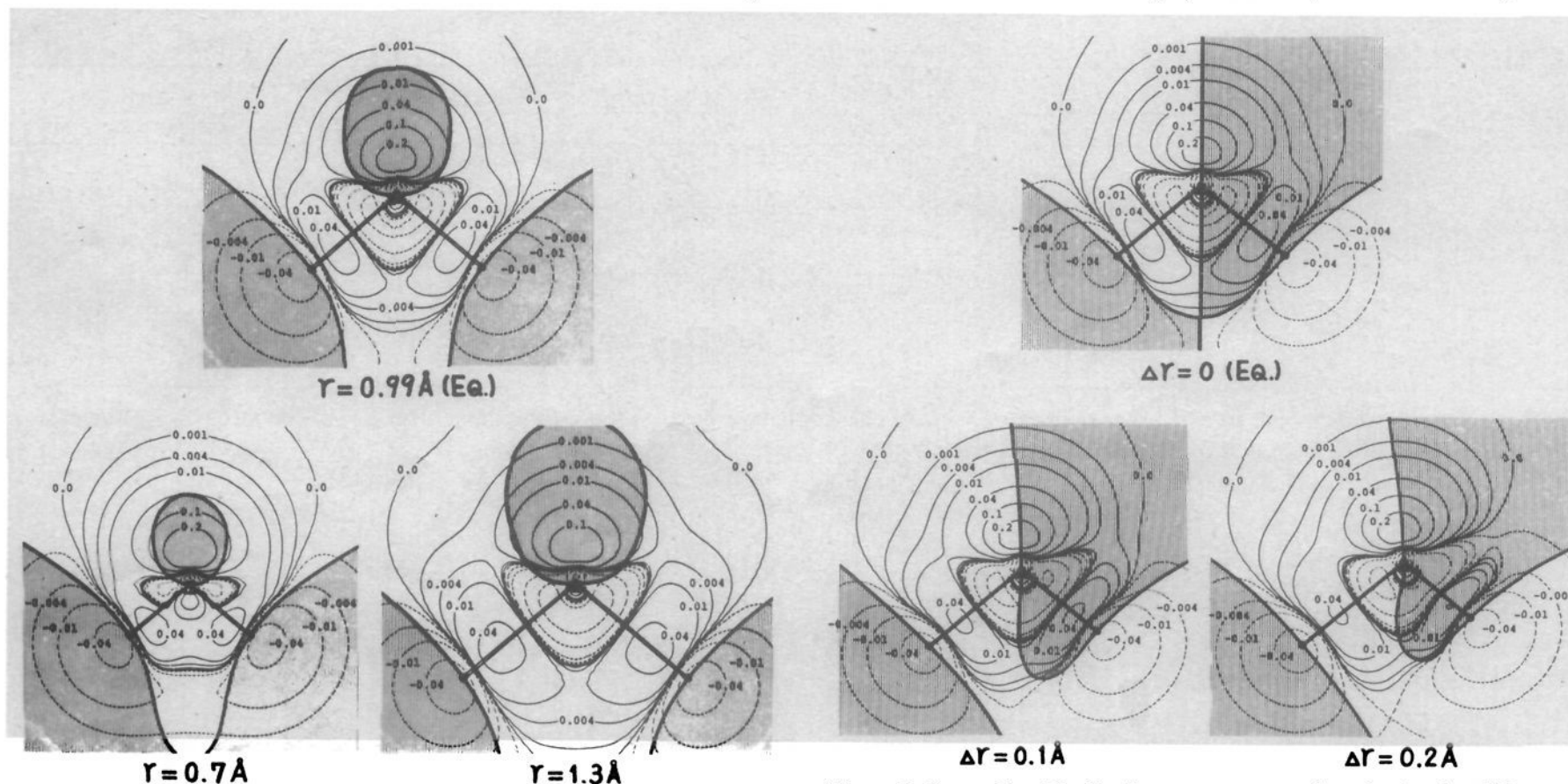


Figure 6. Generalized Berlin diagram superposed on the density difference map in the totally symmetric bond-stretching process in H_2O . The solid and broken lines in the density difference maps mean the increase and the decrease of electron density relative to the atomic density. The shaded parts of the generalized Berlin diagrams are the A region in the totally symmetric stretching mode.

Figure 8. Generalized Berlin diagram superposed on the density difference map in the antisymmetric bond-stretching process in H_2O . The solid and broken lines in the density difference maps mean the increase and the decrease of electron density relative to the atomic density. The shaded parts of the generalized Berlin diagrams are the A region in the antisymmetric stretching mode.

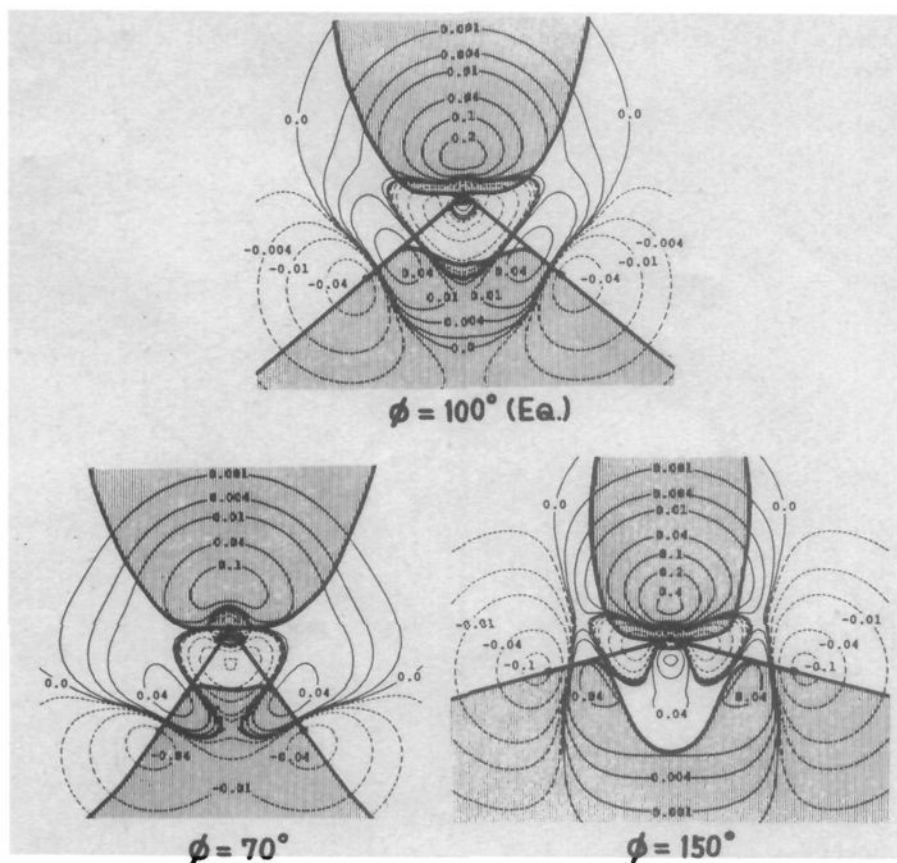


Figure 7. Generalized Berlin diagram superposed on the density difference map in the bending process in H_2O . The solid and broken lines in the density difference maps mean the increase and the decrease of electron density relative to the atomic density. The shaded parts of the generalized Berlin diagrams are the bending region.

ties.²⁴ The A region is shaded in the generalized Berlin diagram. At the equilibrium geometry ($r = 0.99 \text{ \AA}$),²² the force due to the density in the A region is balanced with that due to the density in the R region and the nuclear repulsive force. Actually, the force on H was calculated to be zero from this density.¹⁴ When the O-H bonds are shortened to 0.7 \AA , the electron density in the A region increases particularly in the lone-pair region above O, while the density in the R region

decreases (see the 0.04 contours near the bonds). This density reorganization is reasonable for the elongation of the bonds. When the bonds are elongated to 1.3 \AA , the electron density flows from the A region to the R region and resists the bond-elongation process.

The density behavior along the bending process is depicted in Figure 7. The shaded region is the bending region. At $\phi = 150^\circ$, there is more electron density in the bending region than in the linearizing region. The force on H obtained at $\phi = 150^\circ$ is 0.069 au in the bending direction.¹⁴ At $\phi = 100^\circ$, the bending force balances the linearizing force as understood from the nearly symmetric distribution of the electron density with respect to the O-H axis. The transverse forces on H's vanish at this bond angle.¹⁴ At a smaller angle, $\phi = 70^\circ$, there is more electron density in the linearizing region than in the bending region, especially in the O-H bond region. The force on H calculated at this angle is 0.102 au in the linearizing direction.¹⁴ Consequently, the present analysis is in agreement with the fact that the equilibrium bond angle is evaluated to be 100° from the actual force and energy calculations.^{14,22}

Figure 8 shows the density reorganization for the antisymmetric stretching mode. The shaded part is the A region which works to lengthen the left bond and shorten the right bond.²¹ As the nuclei moves along the mode, the density in the R region increases (see the 0.01 contour near the left bond), while the density in the A region decreases (see the contours near the right bond). The electron density in the lone-pair region above the oxygen slightly rotates toward the left. This rotation throws more electron density into the R region. All of these density behaviors resist the process and work to restore the bonds to the equilibrium.

Summary

In this paper, we have studied the region-functional role of the electron density distribution on the basis of the H-F theorem. We have derived the binding-antibinding diagram for diatomic molecules using the CMN coordinates and compared it with the diagram in the GCN coordinates, i.e., the Berlin diagram.⁵ In the CMN coordinates, the diatomic diagrams are

shown to be classified approximately into two types, AB and AH types. Then, we have explicitly generalized Berlin's region-functional concept of electron density to polyatomic molecules, using the CMN coordinates. The diagrams for other coordinates (GCN and NC) are shown to be obtained as special cases. In the generalized Berlin diagram, the space around a molecule is divided into the accelerating (A) and resisting (R) regions with respect to an internal coordinate of the molecule under consideration. The electron density in the A region accelerates the nuclear rearrangement along the coordinate, while the density in the R region resists it. Therefore, the generalized Berlin diagram defines unambiguously the regions for the electron-cloud preceding and incomplete following. It is suggested that such diagrams are useful in studying the density origin of the nuclear-rearrangement processes. The concept of the generalized Berlin diagram is exemplified for the three internal modes of H₂O molecule. The electron density reorganizations at the nonequilibrium geometries are seen to occur in such a way that facilitates the restoring of the molecule into its equilibrium geometry.

Acknowledgment. We thank Dr. S. Kato and Mr. H. Kobayashi for useful discussions and suggestions. We are also indebted to the referees for some valuable comments. Part of this study has been supported by the grants from the Ministry of Education whom the authors acknowledge.

References and Notes

- (1) H. Hellmann, "Einführung in die Quantenchemie", Deuticke, Vienna, 1937; R. P. Feynman, *Phys. Rev.*, **56**, 340 (1939).
- (2) (a) B. M. Deb, *Rev. Mod. Phys.*, **45**, 22 (1973); (b) B. M. Deb, Ed., "The Force Concept in Chemistry", Van Nostrand-Reinhold, New York, N.Y., in press.
- (3) R. F. W. Bader and A. D. Bandrauk, *J. Chem. Phys.*, **49**, 1653 (1968); R. F. W. Bader, I. Keaveny, and G. Runtz, *Can. J. Chem.*, **47**, 2308 (1969).
- (4) H. Nakatsuji, *J. Am. Chem. Soc.*, **95**, 2084 (1973); **96**, 24, 30 (1974); H. Nakatsuji and T. Koga, Chapter 4 of ref 2b.
- (5) T. Berlin, *J. Chem. Phys.*, **19**, 208 (1951).
- (6) (a) R. F. W. Bader, W. H. Henneker, and P. E. Cade, *J. Chem. Phys.*, **46**, 3341 (1967), and the succeeding papers; (b) B. J. Ransil and J. J. Sinal, *ibid.*, **46**, 4050 (1967); L. A. Curtiss, C. W. Kern, and R. L. Matcha, *ibid.*, **63**, 1621 (1975).
- (7) (a) R. F. W. Bader, *J. Am. Chem. Soc.*, **86**, 5070 (1964); (b) R. F. W. Bader and H. J. T. Preston, *Can. J. Chem.*, **44**, 1131 (1966).
- (8) O. Johnson, *Chem. Scr.*, **6**, 202, 208 (1974).
- (9) L. I. Schiff, "Quantum Mechanics", McGraw-Hill, New York, N.Y., 1955;

- S. T. Epstein, "The Variational Method in Quantum Chemistry", Academic Press, New York, N.Y., 1974.
- (10) A. C. Hurley in "Molecular Orbitals in Chemistry, Physics, and Biology", P.-O. Löwdin and B. Pullmann, Eds., Academic Press, New York, N.Y., 1964; *Proc. R. Soc. London, Ser. A*, **226**, 170, 179, 193 (1954); G. G. Hall, *Phil. Mag.*, **6**, 249 (1961).
 - (11) The equation $f(\text{CMN}) = 0$ means that the accelerations of the nuclei A and B, \mathbf{R}_A and \mathbf{R}_B , are equal in the sense of the dynamical H-F theorem of Kerner (E. H. Kerner, *Phys. Rev. Lett.*, **2**, 152 (1959)). On the other hand, $f(\text{GCN}) = 0$ which gives the Berlin diagram means that the forces on the nuclei, \mathbf{F}_A and \mathbf{F}_B , are equal (see also J. O. Hirschfelder, C. F. Curtiss, and R. B. Bird, "Molecular Theory of Gases and Liquids", Wiley, New York, N.Y., 1964, p 935).
 - (12) It may be interesting to note that the H₂ molecule belongs to the AB type, while the isotope-substituted HD molecule belongs to the AH type. This difference is due to the use of the CMN coordinates where the center of mass is always kept fixed.
 - (13) E. B. Wilson, Jr., J. C. Decius, and P. C. Cross, "Molecular Vibrations", McGraw-Hill, New York, N.Y., 1955; B. L. Crawford, Jr., and W. H. Fletcher, *J. Chem. Phys.*, **19**, 141 (1951).
 - (14) H. Nakatsuji, K. Matsuda, and T. Yonezawa, *Chem. Phys. Lett.*, **54**, 347 (1978); *Bull. Chem. Soc. Jpn.*, **51**, 1315 (1978).
 - (15) (a) R. F. W. Bader and A. K. Chandra, *Can. J. Chem.*, **46**, 953 (1968); A. K. Chandra and K. L. Sebastian, *Mol. Phys.*, **31**, 1489 (1976); (b) H. Nakatsuji, T. Koga, K. Kondo, and T. Yonezawa, *J. Am. Chem. Soc.*, **100**, 1029 (1978); T. Koga, H. Nakatsuji, and T. Yonezawa, *Mol. Phys.*, to be submitted for publication.
 - (16) (a) B. M. Deb, *J. Am. Chem. Soc.*, **96**, 2030 (1974); **97**, 1988 (1975); B. M. Deb, P. N. Sen, and S. K. Bose, *ibid.*, **96**, 2044 (1974); (b) B. M. Deb, *J. Chem. Educ.*, **52**, 314 (1975); B. M. Deb, S. K. Bose, and P. N. Sen, *Indian J. Pure Appl. Phys.*, **14**, 444 (1976).
 - (17) P. E. Cade, R. F. W. Bader, and J. Pelletier, *J. Chem. Phys.*, **54**, 3517 (1971).
 - (18) H. Nakatsuji, *J. Am. Chem. Soc.*, **95**, 345, 354 (1973).
 - (19) O. Goschinski and A. Palma, *Chem. Phys. Lett.*, **47**, 322 (1978).
 - (20) A sketch of the NC coordinates for AH₂ molecules is seen in Figure 1 of C. A. Coulson and B. M. Deb, *Int. J. Quantum Chem.*, **5**, 411 (1971).
 - (21) For the antisymmetric stretching mode, the generalized Berlin diagrams have been obtained from the numerically calculated transformation matrix $\mathbf{G}^{-1}\mathbf{S}\mathbf{M}^{-1}$.
 - (22) The equilibrium geometry of H₂O is taken as $r = 0.99 \text{ \AA}$ and $\phi = 100^\circ$ which is the optimum geometry for the STO-3G basis. The experimental geometry is $r = 0.957 \text{ \AA}$ and $\phi = 104.5^\circ$. See W. A. Lathan, L. A. Curtiss, W. J. Hehre, J. B. Lisle, and J. A. Pople, *Prog. Phys. Org. Chem.*, **11**, 175 (1974).
 - (23) The density of the free oxygen, ρ_O was calculated using the configuration, $(1s)^2(2s)^2(2p_x)^2(2p_y)^2(2p_z)^0$. It is of circular symmetry on the molecular xy plane. The AO exponents used for the free atoms O and H are the same as those used in the molecular calculations (ref 14).
 - (24) The referee has suggested an interesting choice of the reference atomic density of oxygen for the symmetric bond-stretching mode. Namely, since the symmetric dissociation of the ground-state water yields oxygen in the ¹D level, the density corresponding to the configuration $(1s)^2(2s)^2(2p_x)^{5/3}(2p_y)^{2/3}(2p_z)^{5/3}$ may be more suitable for this mode. Note that this configuration has the deficit in density along the C₂(y) axis. He showed that if this $\Delta\rho$ map is used with the generalized Berlin diagram shown in Figure 6, the binding nature in H₂O is more well represented than the present case. We are grateful to the referee for the comments.